Available online at www.sciencedirect.com

SciVerse ScienceDirect

Geochimica et Cosmochimica Acta 90 (2012) 33–46

Geochimica et Cosmochimica Acta

www.elsevier.com/locate/gca

Unusual fractionation of both odd and even mercury isotopes in precipitation from Peterborough, ON, Canada

JiuBin Chen [a,b,*], Holger Hintelmann [b], XinBin Feng [a], Brian Dimock [b]

[a] State Key Laboratory of Environmental Geochemistry, Institute of Geochemistry, Chinese Academy of Sciences, 46 Guanshui Road, Guiyang, GuiZhou 550002, China

[b] Chemistry Department, Trent University, 1600 West Bank Drive, Peterborough, Ontario K9J7B8, Canada

Received 26 October 2011; accepted in revised form 2 May 2012; available online 11 May 2012

Abstract

Once released into the atmosphere, mercury (Hg) is subject to long-range transport and a series of physico-chemical reactions before reentering terrestrial ecosystems. Though impressive progress has been made in understanding all aspects of Hg behavior in the atmosphere, many processes involved in the transformation and deposition of atmospheric Hg remain unidentified and source attribution is still an enormous challenge. Here, we examine the isotopic composition of Hg in precipitation collected during 2010 in Peterborough, ON, Canada and combine data on seasonal variations of mass-dependent (MDF) and mass-independent (MIF) fractionation with meteorological back-trajectory calculations to identify the Hg sources and to decipher Hg atmospheric transformation reactions. All precipitation samples displayed significant MDF (δ^{202}Hg between −0.02‰ and −1.48‰) and MIF of odd isotopes (Δ^{199}Hg varying from −0.29‰ to 1.13‰). We also report for the first time a seasonal variation of MIF of even Hg isotopes (Δ^{200}Hg) in wet precipitation. Our results may suggest that photoreduction in droplets or on the surface layer of snow crystals induces odd Hg isotope anomalies, while mass independent fractionation of ^{200}Hg is probably triggered by photo-initiated oxidation occurring on aerosol or solid surfaces in the tropopause. The observed seasonal variation of even Hg isotope MIF (Δ^{200}Hg decrease with ambient temperature) is possibly a powerful tool for meteorological research and may aid in monitoring related climate changes.

1. INTRODUCTION

Mercury (Hg) is released or re-emitted into the atmosphere by a number of natural or anthropogenic processes and/or emission sources (Mason et al., 1994; Schroeder and Munthe, 1998; Selin, 2009). Once released into the atmosphere (mainly the troposphere), mercury is subject to a variety of physical, chemical and photochemical processes and interactions. Mercury mainly exists in form of three main species in the atmosphere: gaseous elemental Hg (Hg^0), divalent reactive gaseous Hg (RGM) and Hg bound to particulates (Hg_p) (Schroeder and Munthe, 1998). These species are linked to each other by naturally occurring processes such as gaseous and aqueous oxidation of Hg^0 by oxidants (ozone, chlorine, hydroxyl, H_2O_2, etc.), reduction of Hg^{2+} by reductants (CO, SO_2, H_2O_2, etc.), photochemically initiated reduction of Hg^{2+} species and particle adsorption (Hoyer et al., 1995; Schroeder and Munthe, 1998; Lamborg et al., 1999; Lin and Pehkonen, 1999; Lalonde et al., 2002; Ariya et al., 2004; Selin, 2009). The specific pathway that each species experiences in the atmosphere depends on both its physical and chemical characteristics and the redox, environmental and meteorological conditions. Hg^0, which comprises more than 90% of total atmospheric Hg, is relatively inert and has a residence time of about 6 months to 1 year in the atmosphere, allowing long distance transportation (Selin, 2009). However, RGM and Hg_p are much more reactive, readily

* Corresponding author at: State Key Laboratory of Environmental Geochemistry, Institute of Geochemistry, Chinese Academy of Sciences, 46 Guanshui Road, Guiyang, GuiZhou 550002, China. Tel./fax: +86 851 5892669.

E-mail address: chenjiubin@vip.gyig.ac.cn (J.-B. Chen).

0016-7037/$ - see front matter © 2012 Elsevier Ltd. All rights reserved.
http://dx.doi.org/10.1016/j.gca.2012.05.005

deposit and thus dominate in both wet and dry Hg deposition (Lin and Pehkonen, 1999). In general, Hg^0 air–surface exchange is bi-directional. RGM and Hg_p involved in the transfer of Hg from the atmosphere to the earth's surface can be further partially reduced to volatile forms after deposition (Schroeder and Munthe, 1998). Though impressive progress has been made in understanding all aspects of Hg behavior in the atmosphere, many processes involved in the transformation and deposition of atmospheric mercury still remain unidentified and unquantified (Bergquist and Blum, 2009; Selin, 2009). These gaps and uncertainties in the atmospheric Hg cycle are partially linked to the fact that present knowledge is mainly derived from the investigation of tempo-spatial variations of Hg concentrations. New approaches are needed to better understand and quantify Hg dispersion and transformation in the atmosphere.

Recent improvements in multiple-collector ICP-MS instrumentation and sample introduction systems have allowed more accurate and precise measurements of mercury isotope variations (Lauretta et al., 2001; Hintelmann and Lu, 2003; Bergquist and Blum, 2007; Blum and Bergquist, 2007). Preliminary studies have demonstrated both mass-dependent (MDF) and mass-independent fractionation (MIF) of Hg isotopes in natural samples and during some bio-geochemical processes, highlighting the potential of Hg isotope determinations in biochemistry and geochemistry (Bergquist and Blum, 2009; Feng et al., 2010; Point et al., 2011). Because Hg is a bioactive and volatile element with rich redox chemistry, processes involving Hg transformation such as chemical and microbial reduction, demethylation, evaporation, volatilization and condensation create measurable Hg isotope fractionation (Bergquist and Blum, 2009; Sonke, 2011). Photochemical reduction of inorganic mercury (iHg) and methylmercury (MMHg) and liquid–vapor evaporation produce mass-independent fractionation of odd Hg isotopes, which presumably causes the MIF observed in aquatic biological system (Bergquist and Blum, 2007; Biswas et al., 2008; Ghosh et al., 2008; Jackson et al., 2008; Estrade et al., 2009). MIF of odd Hg isotopes is thought to occur due to either the nuclear volume effect (NVE) or the magnetic isotope effect (MIE), with the former causing generally smaller MIF anomalies while the latter induces relatively large MIF of odd isotopes (Bergquist and Blum, 2007, 2009; Schauble, 2007; Sonke, 2011). A detailed description of mechanisms causing MIF of odd Hg isotopes was summarized in Sonke (2011). Though atmospheric deposition is a primary pathway by which Hg enters the terrestrial ecosystem (Mason et al., 1994; Morel et al., 1998), little has been reported on Hg isotopes in precipitation (Bergquist and Blum, 2009; Sonke, 2011). Laboratory experiments indicate that heavier Hg isotopes are preferentially retained in the aqueous solution during aquatic photoreduction and evaporation, while odd Hg isotopes may be enriched or depleted in solution depending on the type of ligand Hg is bound to (Bergquist and Blum, 2007; Zheng et al., 2007; Estrade et al., 2009; Zheng and Hintelmann, 2010b). A recent study reported negative MIF of odd Hg isotopes in lichens and was interpreted to represent atmospheric Hg deposition (Carignan et al., 2009). However, positive MIF of odd Hg isotopes was also determined in both precipitation and ambient air (Gratz et al., 2010; Sherman et al., 2012). These studies also showed positive MIF of even Hg isotopes in precipitation (up to 0.25‰). Neither laboratory experiment nor fieldwork has identified the mechanism or process leading to MIF of even Hg isotopes. Further studies are thus needed to verify this observation and to better understand the Hg isotope composition in the atmosphere.

In this study, Hg isotopic measurements were performed for rain and snow samples collected for the entire year of 2010 using the pre-concentration method developed by Chen et al. (2010). The specific objectives are (1) to investigate systematically the annual variation of Hg isotopic composition in precipitation, (2) to verify and confirm the observation of MIF of both odd and even Hg isotopes reported in previous studies for atmospheric samples, and (3) to better understand the processes inducing both MDF and MIF of Hg isotopes in the atmosphere, especially MIF of even Hg isotopes.

2. ANALYTICAL METHODS

All reagents (HCl, HNO_3, BrCl, L-cysteine, $NH_2OH{\cdot}HCl$, $SnCl_2$) used in this study were analytical grade or prepared under Hg-free condition. All vessels were made of glass or Teflon, and were cleaned with first 1% BrCl, then 50% HNO_3 and a last rinse of de-ionized H_2O before their use. NIST SRM 3133 Hg and UM-Almadén Hg were used as reference standards and measured regularly to control the quality of isotopic measurements.

Sampling was performed in 2010 to monitor annual Hg isotopic variation. Due to low Hg concentration in precipitation (Table 1), only 23 precipitation samples (19 rain and 4 snow samples) had sufficient Hg mass (>5 ng) for an Hg isotope ratio measurement. These samples included 16 one-event samples with water collected from the beginning to the end of a single precipitation event, and 7 multi-event samples with water collected from several rain events with variable collection time. Snow was collected during or immediately after significant snowfall in order to avoid Hg loss after deposition (Lalonde et al., 2003). All samples were collected at a meteorological station located in Peterborough (Ontario, Canada), a mid-latitude location (44.35N, 78.29W) near the Trent University campus, about 5 km north of Peterborough, 130 km northeast of Toronto. There are no Hg sources within the Trent University Campus, nor any known major Hg point sources in the Peterborough region. A tilted "V" type Teflon collector (surface area of about 1 m^2) was used to channel precipitation samples into a pre-cleaned 12 L glass container through a glass funnel. The whole sampling set was stored in dilute HNO_3 solution in the laboratory between two collections. The blank of the whole collecting system is 18 pg ($n = 4$) determined by processing 1 L of de-ionized water. Snow samples were melted in pre-cleaned glass bottles, in a water bath set to 30 °C. Samples were filtered immediately after collection using a four-stage PFA filter system (Savillex) with a final 0.2 μm mixed cellulose membrane filter. The blank of the whole filtration system is 14 pg ($n = 9$). The first 200 ml of filtered water was discarded. After

Table 1
Mercury isotope values and Hg and Na concentrations in precipitation samples from Peterborough (ON, Canada).

ID	Sample	Collection date	T (°C)	Event	Wind direction	Volume (L)	Hg (ng/L)	Na (mg/L)	δ^{199}Hg (‰)	δ^{200}Hg (‰)	δ^{201}Hg (‰)	δ^{202}Hg (‰)	Δ^{199}Hg (‰)	Δ^{200}Hg (‰)	Δ^{201}Hg (‰)
GS($n = 2$)	Greenland Snow[a]					15	0.35		-0.04 ± 0.11	0.29 ± 0.14	0.24 ± 0.17	-1.35 ± 0.18	0.32 ± 0.09	0.91 ± 0.15	1.11 ± 0.06
S1($n = 2$)	Snow1	28/01/10	−6.0	S	NW	6.8	2.02	3.02	-0.30 ± 0.06	1.23 ± 0.12	-0.26 ± 0.01	-0.02 ± 0.07	-0.29 ± 0.04	1.24 ± 0.08	-0.24 ± 0.04
S2($n = 2$)	Snow2	23/02/10	−3.5	S	NW–NE	10.8	2.12	1.33	0.02 ± 0.03	0.53 ± 0.03	-0.67 ± 0.07	-1.36 ± 0.07	0.36 ± 0.01	$1.21 \pm -.10$	0.35 ± 0.02
R1($n = 2$)	Rain1	14/03/10	4.4	S	NE–E	6	3.80	1.45	0.26 ± 0.01	0.53 ± 0.07	0.00 ± 0.05	-0.42 ± 0.07	0.37 ± 0.01	0.74 ± 0.03	0.32 ± 0.10
R2($n = 2$)	Rain2	24/03/10	2.4	M	NE–E	5.6	7.50	0.48	0.84 ± 0.16	0.15 ± 0.10	0.30 ± 0.15	-0.82 ± 0.10	0.97 ± 0.07	0.59 ± 0.01	0.94 ± 0.05
R3($n = 2$)	Rain3	29/03/10	4.3	S	S–SW	3.8	3.43	1.16	-0.17 ± 0.05	0.17 ± 0.04	-0.79 ± 0.16	-0.72 ± 0.16	-0.01 ± 0.04	0.50 ± 0.13	-0.29 ± 0.02
R4($n = 2$)	Rain4	5/04/10	12.7	M	SW	4	9.90	1.01	0.42 ± 0.16	$0,00 \pm 0.09$	0.03 ± 0.05	-0.68 ± 0.03	0.59 ± 0.15	0.34 ± 0.08	0.54 ± 0.07
R5($n = 2$)	Rain5	3/05/10	18.0	S	SW	2	9.24	1.60	0.02 ± 0.10	-0.38 ± 0.05	-0.55 ± 0.12	-1.19 ± 0.10	0.32 ± 0.16	0.22 ± 0.02	0.35 ± 0.04
R6($n = 3$)	Rain6	6/05/10	14.0	S	SW	5.2	6.37	1.01	0.37 ± 0.10	-0.13 ± 0.11	-0.04 ± 0.06	-0.68 ± 0.13	0.54 ± 0.16	0.21 ± 0.04	0.47 ± 0.04
R7($n = 2$)	Rain7	10/05/10	4.6	S	SW–W	6.3	5.64	1.13	0.26 ± 0.10	-0.01 ± 0.09	0.12 ± 0.12	-0.55 ± 0.16	0.47 ± 0.03	0.25 ± 0.08	0.48 ± 0.12
R8($n = 3$)	Rain8	14/05/10	8.8	M	SW	3.7	11.00	0.92	0.18 ± 0.09	-0.35 ± 0.08	-0.33 ± 0.09	-1.25 ± 0.08	0.49 ± 0.07	0.28 ± 0.04	0.61 ± 0.03
R9($n = 2$)	Rain9	3/06/10	20.0	M	NE–NW	10.5	3.15	0.79	0.47 ± 0.03	-0.12 ± 0.01	-0.02 ± 0.16	-1.02 ± 0.02	0.73 ± 0.04	0.39 ± 0.02	0.74 ± 0.16
R10($n = 3$)	Rain10	7/06/10	16.0	M	W	10	4.35	0.95	0.40 ± 0.05	-0.35 ± 0.12	-0.30 ± 0.16	-1.27 ± 0.10	0.72 ± 0.07	0.28 ± 0.11	0.65 ± 0.18
R11($n = 2$)	Rain11	14/06/10	16.0	M	SE	7.5	4.53	1.56	0.35 ± 0.08	0.01 ± 0.09	-0.09 ± 0.11	-0.80 ± 0.09	0.56 ± 0.08	0.42 ± 0.09	0.51 ± 0.11
R12($n = 3$)	Rain12	19/07/10	22.7	S	W	10	6.09	0.53	0.86 ± 0.03	-0.12 ± 0.06	0.21 ± 0.07	-1.04 ± 0.07	1.13 ± 0.02	0.41 ± 0.02	1.00 ± 0.02
R14($n = 2$)	Rain14	29/07/10	21.7	S	W	3	6.24	0.81	0.14 ± 0.06	-0.31 ± 0.09	-0.64 ± 0.14	-1.18 ± 0.10	0.43 ± 0.06	0.28 ± 0.09	0.25 ± 0.14
R15($n = 1$)	Rain15	16/08/10	21.8	S	W	0.9	10.39	0.73	0.35 ± 0.06	-0.50 ± 0.09	-0.42 ± 0.14	-1.59 ± 0.10	0.75 ± 0.06	0.30 ± 0.09	0.78 ± 0.14
R16($n = 2$)	Rain16	23/08/10	18.4	S	W–SW	8.5	8.16	0.76	0.40 ± 0.01	-0.43 ± 0.01	-0.32 ± 0.05	-1.37 ± 0.07	0.75 ± 0.02	0.26 ± 0.02	0.71 ± 0.10
R17($n = 2$)	Rain17	16/09/10	10.3	S	SW	10.4	3.92	0.68	0.45 ± 0.02	-0.25 ± 0.01	-0.17 ± 0.03	-1.03 ± 0.07	0.72 ± 0.04	0.27 ± 0.05	0.61 ± 0.02
R18($n = 2$)	Rain18	21/09/10	19.1	M	NW–SW	3.8	9.75	0.87	0.32 ± 0.03	-0.50 ± 0.05	-0.40 ± 0.03	-1.48 ± 0.06	0.70 ± 0.02	0.24 ± 0.02	0.71 ± 0.02
R19($n = 2$)	Rain19	27/09/10	12.0	S	S	8.2	2.33	0.65	0.20 ± 0.12	-0.37 ± 0.11	-0.52 ± 0.11	-1.20 ± 0.16	0.50 ± 0.07	0.23 ± 0.01	0.38 ± 0.04
R20($n = 1$)	Rain20	25/11/10	−1.0	S	SW–NW	4.4	3.22	1.42	0.11 ± 0.06	0.47 ± 0.09	-0.49 ± 0.14	-1.41 ± 0.10	0.47 ± 0.06	1.18 ± 0.09	0.57 ± 0.14
S3($n = 2$)	Snow3[a]	27/11/10	−2.0	S	W	14	0.35	1.68	0.08 ± 0.08	-0.16 ± 0.08	-0.67 ± 0.08	-1.45 ± 0.09	0.44 ± 0.06	0.57 ± 0.04	0.43 ± 0.01
S4($n = 1$)	Snow4	1/12/10	2.0	S	SW–S	11.3	1.72	0.94	0.45 ± 0.06	-0.24 ± 0.09	-0.18 ± 0.14	-1.10 ± 0.10	0.73 ± 0.06	0.31 ± 0.09	0.65 ± 0.14

n, number of measurements. Error bars are described in detail in the text. W, N, S and E represent respectively west, north, south and east local wind direction. S, single precipitation event; M, multi-event.

[a] Unlike other samples analyzed with one measurement consisted of 5 blocks of 20 cycles, these samples were measured in 5 blocks of 10 due to limited Hg mass.

filtration, samples were acidified with HCl (0.1 M), digested with 0.5% BrCl (0.2 M) and stored at 4 °C. A compacted surface snow sample collected on central Greenland in summer 2009 that likely represented an entire year of snowfall was also analyzed for Hg concentration and isotopic composition. Hg concentration was measured by atomic fluorescence spectrometry (Tekran 2600).

Hg was pre-concentrated from the aqueous matrix according to the protocol developed by Chen et al. (2010). The recovery has been shown to be about 100% and no isotopic fractionation was induced using this method. After cleaning with 0.05% L-cysteine, 4 M HNO_3, and distilled water, a borosilicate glass column charged with 0.5 ml AG 1 × 4 resin was conditioned with 10 ml 0.1 M HCl. Before loading, water samples were acidified to be 0.1 M in HCl and treated with 0.5% BrCl (0.2 M) for at least 12 h to ensure complete organic matter digestion. After having neutralized excess BrCl with $NH_2OH.HCl$ (0.05%), samples were directly introduced onto the column at an average flow rate of 3.5 ml/min, resulting in processing from hours to days depending on the sample volume. After rinsing with 10 ml 0.1 M HCl, Hg was finally eluted with 10 ml 0.5 M HNO_3 containing 0.05% L-cysteine. The final Hg pre-concentration solution was again treated with BrCl for at least 12 h to remove the excess L-cysteine prior to the Hg isotope ratio measurement. Solutions prepared with NIST SRM 3133 Hg and TraceCERT ICP standard Hg (Sigma–Aldrich) were also processed and pre-concentrated to confirm that lab-manipulations do not impact Hg isotopic compositions (Supplementary Table S1).

Hg isotope ratio measurements were performed on a Neptune MC-ICP-MS (Thermo-Fisher, Germany) at Trent University and the technique was described in detail in Chen et al. (2010). Briefly, the previously prepared Hg solution (concentration varied from 0.5 to 2 μg/L) was introduced by a peristaltic pump (at 0.8 ml/min) into the plasma through a continuous flow cold vapor (CV) generation system equipped with an additional Nafion drier tube. The $SnCl_2$ reducing agent was mixed in-line with Hg solution to generate volatile elemental Hg. Tl aerosol produced from an Apex desolvation system was simultaneously introduced into the plasma for mass bias correction. The Faraday cups were positioned to measure five Hg isotopes (^{198}Hg, ^{199}Hg, ^{200}Hg, ^{201}Hg, ^{202}Hg) and two Tl isotopes (^{203}Tl, ^{205}Tl). Due to the limitations of the instrumental collector design, it is not possible to position Faraday cups so that 6 Hg and 2 Tl isotopes can be measured simultaneously. Therefore, ^{200}Hg was measured in this study at the expense of ^{204}Hg in order to verify the observation of $\Delta^{200}Hg$ anomalies in previous studies. The typical ion beam intensity of ^{202}Hg was about 2 V for Hg concentrations of 2 μg/L. The instrumental mass bias was corrected using the modified empirical external normalization (MEEN) method. The MDF of Hg isotopes was expressed using the delta notation ($\delta^x Hg$, in ‰) as defined by the following equation:

$$\delta^x Hg = ((^x Hg/^{198}Hg)_{sample}/(^x Hg/^{198}Hg)_{std} - 1) \times 1000 \quad (1)$$

where $x = 199$, 200, 201, 202, "std" represents the NIST SRM 3133 Hg solution. MIF of Hg isotopes (both odd and even) was defined by the deviation from the theoretically predicted MDF and was expressed as (in ‰):

$$\Delta^{199}Hg = \delta^{199}Hg - 0.252 \times \delta^{202}Hg \quad (2)$$

$$\Delta^{200}Hg = \delta^{200}Hg - 0.502 \times \delta^{202}Hg \quad (3)$$

$$\Delta^{201}Hg = \delta^{201}Hg - 0.752 \times \delta^{202}Hg \quad (4)$$

Our repeated measurements of UM-Almadén Hg gave a long-term ($n = 53$) average $\delta^{202}Hg$ value of -0.56 ± 0.10‰, consistent with previous reported values (Bergquist and Blum, 2007; Blum and Bergquist, 2007). The obtained uncertainties (2 standard deviations, 2σ) were 0.06‰, 0.09‰, 0.14‰, 0.10‰, 0.04‰, 0.03‰, 0.06‰ for $\delta^{199}Hg$, $\delta^{200}Hg$, $\delta^{201}Hg$, $\delta^{202}Hg$, $\Delta^{199}Hg$, $\Delta^{200}Hg$, $\Delta^{201}Hg$, respectively, and were considered as the typical external uncertainties for samples measured only once due to limited sample volumes. If sufficient sample was available, the uncertainty was calculated as the 2σ external standard deviations of multiple measurements (Table 1).

3. RESULTS AND DISCUSSION

3.1. Annual mercury concentration and isotopic variation in precipitation

Volume weighted mercury concentrations in all wet precipitation samples varied from 0.35 ng/L (S3) to 11 ng/L (R8), with an average value of 5.44 ng/L (Table 1). The lowest value of 0.35 ng/L was also found in the Greenland snow. These Hg concentrations were similar to or slightly lower than those previously reported for the same region (Hoyer et al., 1995; Landis and Keeler, 2002; Lalonde et al., 2003; Gratz et al., 2010), and displayed a general qualitative agreement with the data measured by the National Atmospheric Deposition Program (http://nadp.sws.uiuc.edu) at the station Egbert ON07 (Supplementary Fig. S1).

All samples, especially one-event samples, displayed a clear seasonal variation in Hg concentration (Fig. 1a), with lower values determined in snow or rain samples collected in winter and higher in late spring or summer. For one-event samples (solid points), this seasonal variation can also be expressed as a correlation ($y = 0.24x + 2.52$, $r^2 = 0.67$, Supplementary Fig. S2) between Hg concentration and ambient temperature, expressed as the mean value of the 3 days leading up to sample collection. All precipitation samples displayed negative $\delta^{202}Hg$ values, with the highest value of −0.02‰ measured in the snow sample S1 and the lowest value of −1.48‰ in the rain sample R17 (Table 1 and Fig. 1b). $\delta^{202}Hg$ values did not display significant seasonal variations and did not correlate with temperature.

Significant MIF of odd Hg isotopes was determined in all precipitation samples, with $\Delta^{199}Hg$ varying from −0.29‰ to 1.13‰ (Table 1 and Fig. 1c). $\Delta^{201}Hg$ showed similar variation as $\Delta^{199}Hg$. Except for the snow S1 and the rain R3 that had slightly negative or near zero $\Delta^{199}Hg$ values (Table 1 and Fig. 1c), all samples displayed positive MIF of odd Hg isotopes (0.32–1.13‰). $\Delta^{199}Hg$ varied

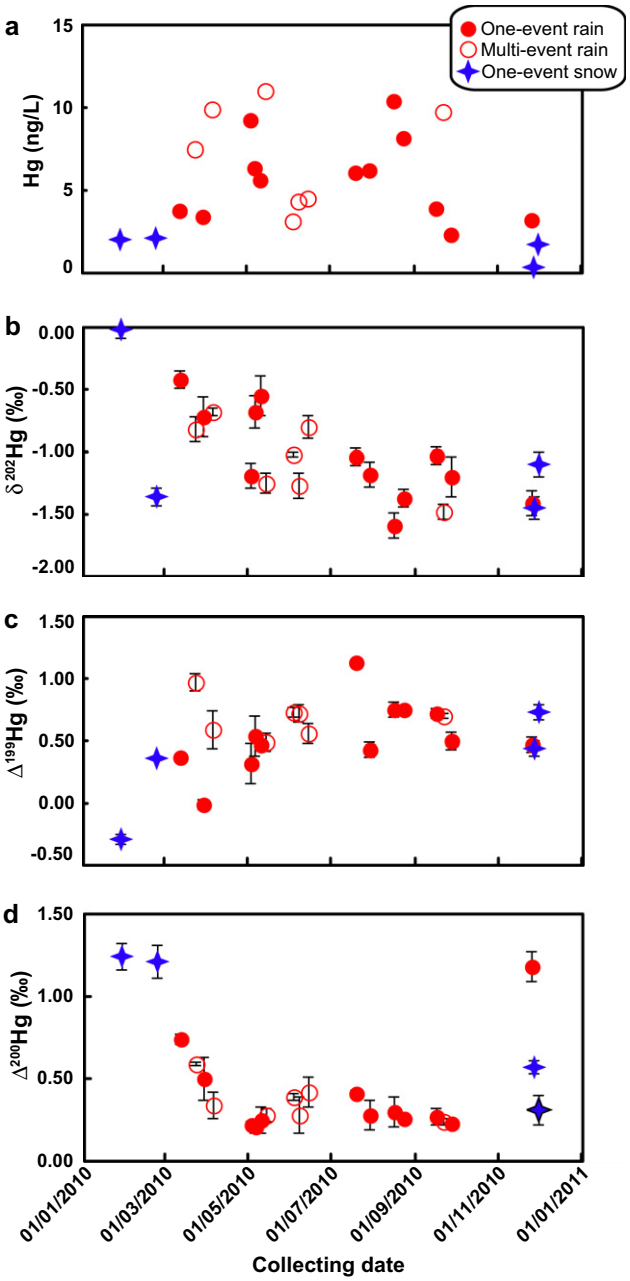

Fig. 1. Annual variation of Hg concentration, δ^{202}Hg, Δ^{199}Hg and Δ^{200}Hg. Samples include 12 one-event rains (red points), 7 multi-event rains (red circles) and 4 one-event snows (full stars) and were collected in 2010 in Peterborough, Ontario, Canada. Error bars are 2σ external standard deviations for samples with multiple measurements, or 0.10‰, 0.04‰, 0.03‰, respectively, for δ^{202}Hg, Δ^{199}Hg and Δ^{200}Hg of samples measured only once. (For interpretation of the references to color in this figure legend, the reader is referred to the web version of this article.)

seasonally and slightly increased with temperature ($y = 0.017x + 0.362$, $r^2 = 0.28$, Fig. 2).

Especially noteworthy in this study is the observation that all rain and snow samples displayed significant positive Δ^{200}Hg values. A total variation of 1.03‰ was observed, with the lowest value of 0.21‰ measured in the rain R6 and the highest value of 1.24‰ in the snow S1 (Table 1 and Fig. 1d). Δ^{200}Hg values showed a seasonal variation: the highest value was found for the snow S1 collected in January, Δ^{200}Hg then decreased sharply to 0.22‰ in May, fluctuated between 0.21‰ and 0.42‰ during summer and fall, and increased again to 0.57‰ in December (Fig. 1d). According to the relationship between Δ^{200}Hg and temperature (Fig. 2), two groups of samples can be distinguished: the first group was composed of snow samples and cold rain samples, where Δ^{200}Hg values varied between 1.24‰ and 0.25‰, and displayed a decrease with increasing temperature from below freezing to about 5 °C; the second

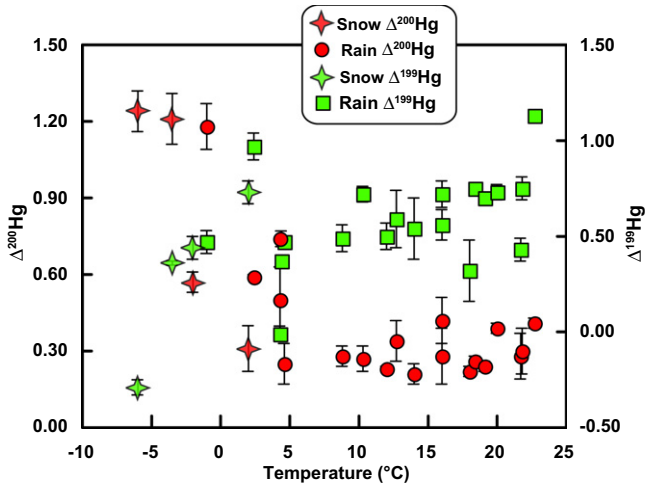

Fig. 2. Δ^{199}Hg (green points) and Δ^{200}Hg (red points) as a function of temperature. Error bars are 2σ external standard deviations for samples with multiple measurements, or 0.04‰ and 0.03‰, respectively, for Δ^{199}Hg and Δ^{200}Hg of samples measured only once. (For interpretation of the references to color in this figure legend, the reader is referred to the web version of this article.)

group included rain samples collected at relatively higher temperature (between 5 and 25 °C), with Δ^{200}Hg varying between 0.21‰ and 0.42‰.

3.2. Long-range transportation effects on Hg budget in precipitation

Local sources may directly contribute to Hg in precipitation. The Peterborough city with a population of about 75,000 is located in the Kawartha tourist region, where the number and the extent of different types of Hg sources are very limited, suggesting that local contributions are also very limited and Hg determined in our precipitation samples is thus more likely derived from long-range transport.

Transport models are very useful for back-tracking the long-range Hg trajectory within air masses and for tracing potential Hg sources (Jaffe et al., 2005; Selin and Jacob, 2008). We calculated kinematic back-trajectories of air masses using NOAA-HYSPLIT model for one-event samples (Draxler and Rolph, 2003; Jaffe et al., 2005). Back trajectories of air masses with initial starting heights of 500, 1000, and 3000 m above ground level (AGL) were monitored for investigating vertical movements of air masses and back-trajectories of 6000 m AGL elevation were also calculated for investigating the possible influence of stratosphere incursion (Lindberg et al., 2002; Stohl et al., 2003; Lyman and Jaffe, 2012). By combining the observation and the local meteorological data (i.e. wind direction, cloud top height, etc.) reported by Environment Canada for the sampling station (Table 1), three main meteorological wind regimes were determined for our sampling station: south (south-west, south-east), west (north-west) and north wind. In general, the south and west winds predominated from late spring to early autumn, while the influence of north wind events increased in the winter. These three main wind regimes may transport Hg with different distances from three directions to our sampling site. Though Hg can undergo variable physio-chemical reactions among different phases during transport, these three main wind regimes may still give some useful information about the origin of Hg in precipitation samples in Peterborough. We will discuss this in detail.

3.2.1. Southern contribution of Hg transported over moderate distance

When wind from the south dominates, the Hg budget in precipitation in Peterborough may be impacted by the Greater Toronto Area (GTA), the nearest location with potentially significant RGM emission (5–100 kg/year in different sectors) (CAMNet, Environment Canada). However, compared to the number and the extent of emission sources in the Northern USA and the Great Lakes region, the contribution from the GTA may be not significant. High anthropogenic Hg emissions were reported from a combination of sources including coal-fired power plants, waste incineration, fuel combustion, metallurgical and manufacturing industries in New York, the Great Lakes and the Chicago industrial regions, with an RGM emission rate of about 50–160 g/km^2/year (Kim et al., 2005; Travnikov, 2005; Selin and Jacob, 2008; Selin, 2009; US EPA). Given that the atmospheric residence time of RGM is approximately several weeks and that RGM is readily incorporated into droplets or adsorbed onto particles (Morel et al., 1998; Selin, 2009), these high anthropogenic emissions may have an important impact on local dry and wet deposition (Kim et al., 2005; Selin and Jacob, 2008; Durnford et al., 2010; Gratz et al., 2010). Previous studies have reported that Hg contributions from the Northern USA tend to dominate Hg deposition in subarctic regions and overwhelmingly at mid-latitude stations (Landis and Keeler, 2002; Stohl et al., 2003; Durnford et al., 2010). Hg originating from the Northern USA may thus impact the precipitation in the Peterborough region after moderate long-range transport, especially during late spring to early autumn, when south and south-west winds dominate.

The contribution of Hg from the Northern USA is also supported by the NOAA-HYSPLIT model and local

meteorological data. In general, the low elevation (500 m, 1000 m AGL) air masses associated with precipitation samples S1, R1, R3, R6 and R7 came mainly from or passed through the Northern USA, in south and south-west dominated wind events. For two typical samples S1 and R3, their low elevation air masses stayed 2–4 days in the Northern USA and the Great Lakes region before arriving at the sampling station (Supplementary Fig. S3). These air masses may incorporate Hg emitted (mainly in RGM form) from this region and transport it northward to the Peterborough region. Although low elevation air masses for samples R1 and R6 came mainly from the east and west, their 6000 m AGL air masses sunk towards the earth surface (<500 m) when approaching the sampling station (Fig. S4). Hg emitted in the Northern USA was possibly scavenged into the descending cloud droplets, giving these two samples a Hg isotope signature characteristic for samples originating in the Northern USA.

Little data is available for isotopic composition of anthropogenic Hg sources in the Northern USA. Since these anthropogenic sources were variable and their distribution is complicated, we were not able to collect and measure isotopic composition of Hg from these sources. However, a recent study reported an average δ^{202}Hg value of $-0.32‰$ for precipitation in this region (Gratz et al., 2010). This value may represent the typical mean isotopic composition of RGM in the Northern USA and the Great Lakes region and is very close to values measured in samples with south-dominated wind (e.g. S1, R3, R1, R6, Fig. 3). This isotopic similarity may suggest a contribution of RGM originating from the Northern USA to Hg in some

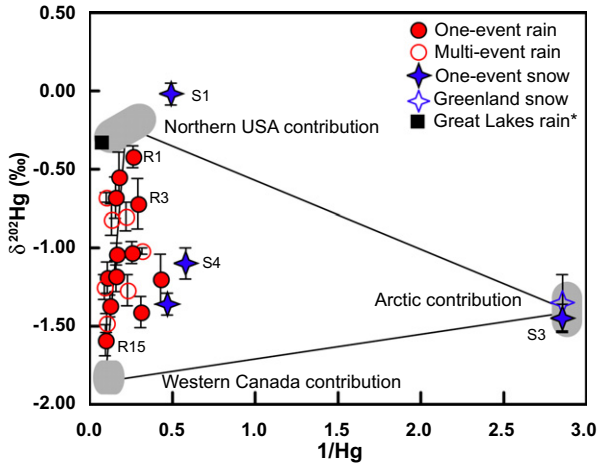

Fig. 3. Mixing diagram showing contribution of three proposed end-members. All data points can be explained by mixing of three main sources: moderate-range transport of Hg from the North USA and Great Lakes region, long-range transport of Hg from western Canada and central North America, and the Arctic. The result is consistent with a meteorological model. Average values (black square) of precipitation in the Great Lakes region are used to represent typical Hg isotopic composition of the Northern USA (Gratz et al., 2010). The Greenland snow (empty star) may support the idea of the direct arctic contribution. *Data from Gratz et al. (2010).

samples after a moderate transport distance. Though variable physico-chemical processes may fractionate Hg isotopes in the atmosphere, the δ^{202}Hg signatures would not be significantly modified for RGM transported from the emission in the Northern USA to deposition due to the short transport distance (thus reaction time). This idea is supported by the similarity of Δ^{200}Hg values (around $0.21‰$) of samples (i.e. R19, R5, R6) collected during south-wind dominated events with those reported in precipitation from the Great Lakes region (Gratz et al., 2010). The same study also reported a local source contribution to the overall Hg budget in precipitation (Gratz et al., 2010; Sherman et al., 2012). We therefore suggest that the important emission in the Northern USA and the Great Lakes region is a principal contributor to Hg in precipitation samples collected during south-wind events.

3.2.2. Long-range Hg transport from the western continent

Unlike S1 and R3, samples S2, R15, R16, R19 and R20 have more negative δ^{202}Hg values close to $-2.00‰$ (Table 1 and Fig. 3). Since Hg derived from southern regions generally displayed higher δ^{202}Hg (close to $0.00‰$), the more negative δ^{202}Hg value may suggest the integrated isotopic composition of Hg transported from western, northern or eastern directions to our sampling station. The HYSPLIT model suggested that low elevation air masses of samples S2, R15 and R16 mainly came from the west. Since the northwestern region near Peterborough is mainly forested land, where human activities are very limited, local source contribution to Hg in our samples is likely negligible. We thus anticipate a contribution of long-range Hg transport (both vertical and horizontal) in air masses arriving from the west and the center of the American continent. However, compared to the Northern USA and the Great Lakes region, point sources of Hg in western Canada and central North America are less significant and the direct contribution of RGM from these regions to the Peterborough area may thus be limited. Considering that ambient atmospheric Hg is predominantly Hg^0, while Hg in precipitation is primarily RGM and Hg_p, Hg in our precipitation samples collected in west-wind dominated events is probably derived from the accumulation of RGM and Hg_p in droplets formed in the atmosphere during transport.

Previous studies demonstrated that maximum Hg concentrations tend to be found in the mid troposphere in the 50–60 latitude band in North America and may be linked to the northern Pacific or even Asian Hg emissions (Strode et al., 2008; Durnford et al., 2010). Trajectory analysis and satellite data suggested that air masses originating from Asia might move northeastward across the Pacific, be lifted in warmer air parcels into the middle and upper troposphere and subsequently exported to North America (Jaffe et al., 2005; Kim et al., 2005; Strode et al., 2008; Durnford et al., 2010). Considering the lifetime and the characteristics of different atmospheric Hg species, Asian RGM would not be directly transported to North America. Instead, Hg from Asian sources in North America would be dominated by Hg^0. Elemental Hg could be further oxidized to RGM (or Hg_p), readily scavenged into cloud droplets during transport, and possibly present an important

contribution to Hg in final precipitation samples. Asian influence may increase in spring and summer, but decrease in autumn and winter (Jaffe et al., 2005; Strode et al., 2008). The observed increase in Hg concentration with temperature (Fig. 1a and Fig. S2) may suggest an association with increasing contributions from Asian Hg sources. Hg transported in west wind events may combine with Hg emitted in North America, which could lead to even higher Hg concentrations in some precipitation samples originating from western Canada (Fig. 3).

Laboratory experiments of aqueous Hg (and MMHg) photo-reduction and Hg^0 evaporation showed that lighter Hg isotopes preferably evade into air, implying more negative δ^{202}Hg values in atmospheric Hg (Bergquist and Blum, 2007; Estrade et al., 2009; Zheng and Hintelmann, 2009). Negative δ^{202}Hg was determined in samples potentially impacted by atmospheric Hg deposition, including sediments, peat, mosses, lichens, rain and snow (Biswas et al., 2008; Ghosh et al., 2008; Carignan et al., 2009; Estrade et al., 2009; Gratz et al., 2010; Sherman et al., 2010, 2012). The complex processes occurring in the atmosphere after Hg is emitted and again deposited make it very difficult to relate the Hg isotopic signatures in our samples to specific sources. Unfortunately, in the absence of Hg isotopic data for air in Asia or western and central North America and lacking studies on the effect of atmospheric reactions on Hg isotope fractionation, we are not able to evaluate the exact contributors of Hg in samples collected in west-wind dominated events. More systematic work is thus needed to identify possible sources and to better understand Hg isotopic fractionation induced by atmospheric processes.

3.2.3. Arctic contribution

The above-discussed two main contributions are further supported by Fig. 3, where data points of all rain samples and most snow samples define a linear relationship. However, snow samples (especially S3) and several cold rain samples (i.e. R19, R20) deviate from the linear relationship. Another contribution is thus needed to explain the entire distribution of data points. As all deviating samples were collected in winter, early spring or late autumn, when southward cold weather dominated, cold air mass originating in the Arctic region may contribute to Hg in these samples. In winter, the lower tropospheric circulation is dominated by high pressures over the Arctic and low pressures over the northern American continent. Air masses are thus forced southward, resulting in a net transport of arctic Hg over North America to our sampling site (Macdonald et al., 2005). The transport of contaminants from the north weakens in summer due to the disappearance of high-pressure cells. HYSPLIT data also show clearly the impact of Arctic air masses on 500 m AGL, especially for snow sample S3, but also for S2, S4 and the cold rain samples R19 and R20. Moreover, the compacted surface snow sample collected on central Greenland in summer 2009, likely represented an entire year of snowfall, had similar Hg concentration (0.35 ng/L) and isotopic composition (−1.35‰) as S3 (Table 1), providing additional support to the idea of arctic contribution to our snow and cold rain samples. However, Hg in the arctic atmosphere may originate from a combination of Northern European, Russian, Asian or even North American contributions and the re-emission of previous deposition may also fractionate Hg isotopes (Macdonald et al., 2005; Sherman et al., 2010). More work is thus needed to decipher the exact contributing sources and related isotopic fractionation during Hg cycling in the arctic and subarctic region.

In conclusion, we suggest that Hg in local precipitation is mainly derived by long-range transport from northern USA, western Canada and the Arctic, with the former two sources dominating in summer, while arctic sources are more important in winter. Since atmospheric processes may fractionate Hg isotopes during transportation, we do not expect that initial source signatures are necessarily preserved during long-range transport. However, we would expect that the degree of fractionation (if indeed occurring) between source and receptor sites is similar for similar transport histories. Combining the final isotopic signatures in precipitation samples and tracing air mass trajectories by use of the meteorological data results in a coherent model suggesting that Hg source regions are identifiable with the proposed three-contributor model (Fig. 3). Hg found in a single sample may be a combination of these three contributions, e.g. Fig. S4 illustrates the suggested combined impact of the Arctic and the Northern USA on rain R1.

3.3. Mass-independent fractionation of odd Hg isotopes

All our samples displayed significant MIF of odd Hg isotopes (Table 1). Except for S1 and R3, all samples had positive Δ^{199}Hg values (Fig. 4). This is in contrast to predictions based on measured negative Δ^{199}Hg in mosses and lichens, which were thought to be the result of atmospheric Hg deposition (Ghosh et al., 2008; Carignan et al., 2009; Estrade et al., 2009). Negative Δ^{199}Hg values were also expected as a result of aqueous photoreduction of Hg^{2+} (MMHg) and Hg^0 evaporation, in which heavier (i.e. ^{202}Hg) and odd (^{199}Hg, ^{201}Hg) Hg isotopes remain

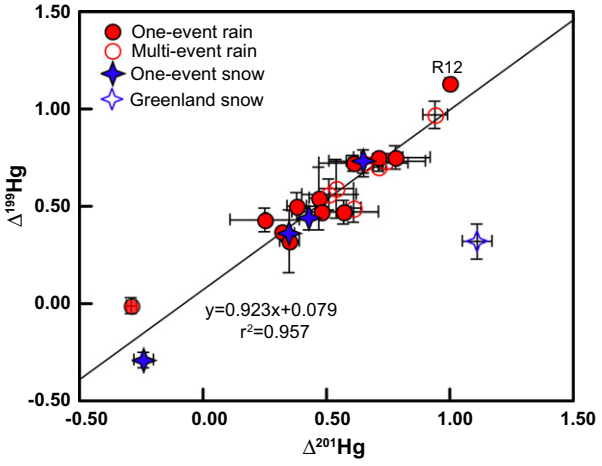

Fig. 4. Mass-independent fractionation of odd Hg isotopes in precipitation samples. The slope of 0.92 defined by all samples is consistent with MIF of odd Hg isotopes derived from photochemical reactions as a result of the magnetic isotopic effect.

preferentially in solution (Bergquist and Blum, 2007; Ghosh et al., 2008; Carignan et al., 2009; Estrade et al., 2009; Zheng and Hintelmann, 2009). However, a recent study showed that aqueous photo-reduction might also lead to enrichment of the odd isotopes in the vapor depending on the ligands (i.e. cysteine), to which Hg is bound to (Zheng and Hintelmann, 2010b). These inconsistent results make it difficult to predict the isotopic composition, especially the odd Hg isotope anomalies in the atmosphere.

Previous studies have suggested that the relationship between the MIF of the two odd Hg isotopes can be used to distinguish among specific photoreduction processes and allow for the identification of specific chemical pathways (Bergquist and Blum, 2007; Estrade et al., 2009; Zheng and Hintelmann, 2009). The mechanisms producing MIF in odd Hg isotopes are not fully understood. However, the magnetic isotope effect (MIE) and nuclear volume effect (NVE) are thought to be important mechanisms causing significant MIF of the odd Hg isotopes (Bergquist and Blum, 2007; Sonke, 2011). The NVE theoretically induces Δ^{199}Hg/ Δ^{201}Hg ratios between 1.60 and 1.65, which is consistent with recent laboratory experiments of liquid–vapor evaporation, Hg^{2+} reduction in the dark, and Hg^{2+}–thiol complexation (Estrade et al., 2009; Wiederhold et al., 2010; Zheng and Hintelmann, 2010a). The MIE can produce large MIF of odd Hg isotopes with Δ^{199}Hg/ Δ^{201}Hg ratios between 1.0 and 1.3, and is deemed to be responsible for MIF of odd isotopes during aqueous Hg photoreduction (Bergquist and Blum, 2007; Sonke, 2011). In this study, all precipitation samples displayed a Δ^{199}Hg/Δ^{201}Hg ratio of 0.92 ± 0.19 (Fig. 4), being undistinguishable from that observed in arctic snow samples (1.07) and atmospheric samples in the Great Lakes (0.89) and the Florida (1.05) regions. All of these values are close to a Δ^{199}Hg/Δ^{201}Hg of 1, which is considered consistent with MIF caused by MIE, but different from that produced by NVE (Bergquist and Blum, 2007; Schauble, 2007; Sherman et al., 2010; Zheng and Hintelmann, 2010a; Sonke, 2011). The MIF of odd Hg isotopes determined in our samples is likely derived from photochemical reactions as a result of the magnetic isotope effect.

Most aqueous photoreduction experiments propose that odd and heavier isotopes would preferentially remain in solution (Bergquist and Blum, 2007; Zheng and Hintelmann, 2009). With the presence of organic matter in cloud droplets, such photoreduction may occur in the atmosphere and thus induces an enrichment of odd Hg isotopes in oxidized Hg species in water droplets. The significant positive Δ^{199}Hg determined in rain samples of this study may thus result from the photoreduction of Hg in water droplets, as suggested for precipitation in the Great Lakes and the Florida regions (Gratz et al., 2010; Sherman et al., 2012). As these positive Δ^{199}Hg anomalies resulted from photoreduction in the atmosphere, large values of Δ^{199}Hg may imply an extended fractionation in water droplets subject to long-range transport. The odd isotope enrichment derived from aqueous photoreduction and Hg^0 evaporation in the atmosphere would be accumulative, especially in summer with intensive sunlight irradiation. Δ^{199}Hg in final rainfall thus increases with time of residence in the atmosphere and with transportation distance. Compared to the relatively lower Δ^{199}Hg values (<0.70‰) reported for rain samples impacted by local Hg sources (Gratz et al., 2010; Sherman et al., 2012), the higher Δ^{199}Hg values (up to 1.13‰) determined in this study may result from the extended photoreduction during long-range transportation. Fig. 5 shows an inverse relationship ($r^2 = 0.25$) between Δ^{199}Hg and δ^{202}Hg for all precipitation samples. Samples with more positive Δ^{199}Hg values (i.e. R12, R15, R16) displayed relatively negative δ^{202}Hg values (<−1.00‰), while samples S1, R1 and R3 had higher δ^{202}Hg values but lower Δ^{199}Hg. This inverse relationship resulted probably from extended photoreduction of Hg in droplets during long-range transport. Since progressive photoreduction reactions should induce a positive relationship between Δ^{199}Hg and δ^{202}Hg, the opposite observation in Fig. 5 may be explained by differences in underlying source MDF isotope signatures. Though more studies are needed to identify these different processes, our results support earlier suggestions that MDF and MIF Hg isotope signatures each carry specific information (Sonke, 2011).

In contrast to experimental results of aqueous Hg^{2+} photoreduction and Hg^0 evaporation, a depletion of odd Hg isotopes in residual snow was found in a chamber experiment with drifted arctic snow and was suggested to be related to photochemical processes involving Hg-halogen radical-pairs in the quasi-liquid surface of snow crystals (Sherman et al., 2010). We suggest that these heterogeneous processes occurred also in atmospheric snow and thus may explain the negative Δ^{199}Hg found for snow S1 in this study. Halogen-involved reactions are typically important in arctic environments and in the marine boundary layers (Lalonde et al., 2002; Douglas and Sturm, 2004; O'Dowd and de Leeuw, 2007; Sherman et al., 2010). Sea–salt parti-

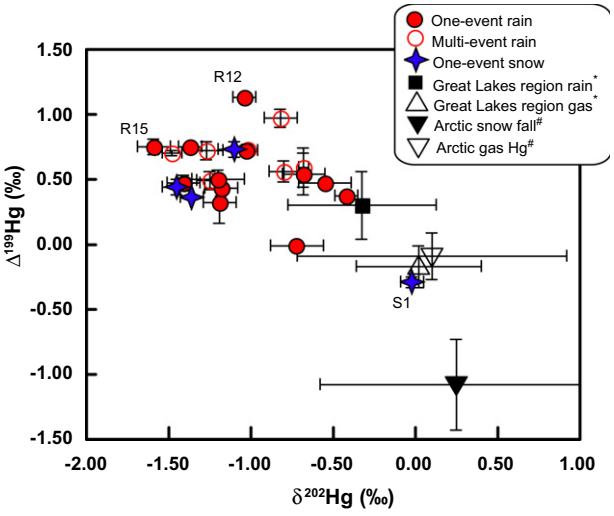

Fig. 5. Inverse relationship between MIF of odd isotopes and MDF of Hg isotopes. Mean values of Hg concentrations and Hg isotopic compositions of arctic air and snow fall (Sherman et al., 2010), and of gaseous Hg and precipitation in the Great Lakes region (Gratz et al., 2010) were also plotted. *Data from Gratz et al. (2010). #Data from Sherman et al. (2010).

cles derived from sea spray are the dominant source for the global aerosol inventory including halogens and related elements such as Na (Douglas and Sturm, 2004; de Caritat et al., 2005; O'Dowd and de Leeuw, 2007). Fig. 6a shows an inverse correlation between Δ^{199}Hg and Na. Samples collected in cold weather (i.e. S1, S2, S3, R1, R20) displayed relatively higher Na concentrations (>1 mg/L) and lower Δ^{199}Hg (<0.50‰). These samples may have a significant contribution of Arctic snow and/or frozen aerosols with mainly sea–salt origin. The lower Na concentrations in samples (i.e. R12, R15, R16) with higher Δ^{199}Hg (Fig. 6a) suggests that arctic contributions were limited. This is consistent with meteorological data. The inverse correlation between Δ^{199}Hg and Na concentration thus supports the notion that heterogeneous processes in or on atmospheric snow aerosols may be responsible for negative Δ^{199}Hg found in snow samples such as S1.

3.4. Conceptual model for ^{200}Hg anomalies in precipitation samples

We will refer in the following to ^{200}Hg anomalies, a term first coined by Gratz et al. (2010), who observed for precipitation samples that Hg isotope ratios of the three even isotopes ^{198}Hg, ^{200}Hg and ^{202}Hg did not fit linearly onto a three isotope plot. Since the $^{202/198}$Hg ratio is conventionally used as the reference ratio, they declared that ^{200}Hg behaves differently. However, one cannot identify which of the three isotopes is anomalous. In fact, one might suspect that all even isotopes are subject to the same fractionating process and thus, are subject to fractionation that does not change linearly with mass. While the measurement of ^{204}Hg may have helped in answering this question, we unfortunately were not able to measure this isotope simultaneously. Nevertheless, in the absence of a clearer understanding of the underlying mechanism and for the purpose of the following discussion, we also pretend that the observed deviations in our study are due to anomalous behavior of ^{200}Hg, but it should be understood that any or all of the even isotopes may be contribute to the observed effect. Clearly, the Hg isotope system is extremely complex and we are a long way from fully understanding its intricacies.

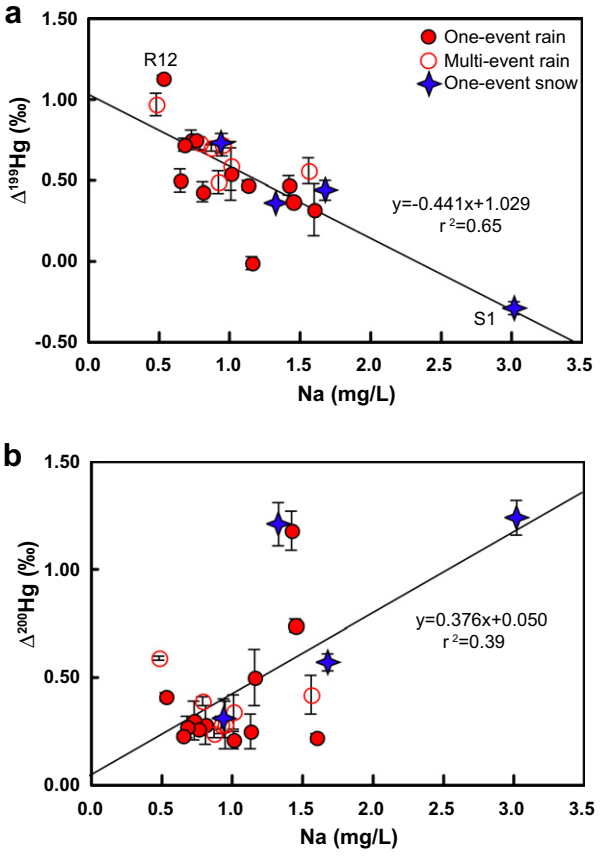

Fig. 6. Relationships between MIF of odd (a) and even (b) Hg isotopes and Na concentrations in precipitation samples. Error bars represent 2σ external standard deviations for samples with multiple measurements, or ±0.04‰ and ±0.03‰ for Δ^{199}Hg and Δ^{200}Hg of samples measured only once, respectively.

In this study, we report for the first time a seasonal variation of Δ^{200}Hg in natural precipitation samples (Table 1). Our results are consistent with the so far unexplainable observation of MIF of ^{200}Hg reported in precipitation (Gratz et al., 2010; Sherman et al., 2012). To ensure that the analytical protocol does not generate MIF of ^{200}Hg, experiments with NIST SRM 3133 Hg and TraceCERT ICP Hg standard solutions were performed using the same pre-concentration and measurement procedure as for all precipitation samples. No MIF of ^{200}Hg was ever determined in these processed standards (Supplementary Table S1). Moreover, long-term regular measurements (several years) in our group using NIST SRM 3133 and Almadén Hg never displayed significant MIF of ^{200}Hg. This strongly suggested that MIF of ^{200}Hg was not derived from lab manipulation or the isotopic measurement itself. To our knowledge, MIE and NVE would not induce significant MIF of even Hg isotopes (Bergquist and Blum, 2007; Gratz et al., 2010; Zheng and Hintelmann, 2010b), the only other mechanism potentially causing Δ^{200}Hg anomalies is photochemical self-shielding, which fractionates Hg isotopes according to their relative abundances (Mead et al., 2010). Since this effect has been postulated to create MIF in all Hg isotopes, we also calculated $\Delta^{200/202}$Hg based on $\delta^{198/202}$Hg and $\Delta^{198/200}$Hg based on $\delta^{202/200}$Hg to explore possible, but hidden alternate systematics. However, both approaches show significant seasonal variations as Δ^{200}Hg (figures not shown). Unfortunately, it was not possible to measure ^{204}Hg in these experiments, due to instrumental collector design limitations, and re-analysis of samples using a cup configuration, which includes ^{204}Hg, was also not possible because all sample material was exhausted. Up to now, the exact theoretical mechanism producing Δ^{200}Hg anomalies remains unknown. We are unaware of any laboratory experiments producing clear ^{200}Hg anomalies. Instead, we propose a conceptual model to explain the observed MIF of ^{200}Hg in our precipitation samples.

Significant MIF of odd Hg isotopes has been determined in terrestrial geological and biological samples and was induced in laboratory experiments, while no ^{200}Hg anomalies

have been found in these studies (Bergquist and Blum, 2007; Estrade et al., 2009; Zheng and Hintelmann, 2009; Sonke, 2011). We argue that the Δ^{200}Hg anomalies were produced in the atmosphere. Though MIF of both odd and even Hg isotopes have been determined in atmospheric samples (Gratz et al., 2010; Sherman et al., 2010), the fact that Δ^{199}Hg and Δ^{200}Hg displayed contrasting seasonal (thus with temperature) variations (Figs. 1 and 2 and Supplementary Fig. S5) may suggest that the MIF of odd and even isotopes is the result of different (photo)chemical reactions. The Hg inventory for surface evasion is mainly composed of elemental mercury (Mason et al., 1994; Schroeder and Munthe, 1998; Selin, 2009). Two studies have reported slightly negative or close to zero Δ^{200}Hg values (−0.11‰ to 0.01‰) of ambient gaseous Hg in the Arctic and in the Great Lakes region (Gratz et al., 2010; Sherman et al., 2010). The positive Δ^{200}Hg found in our wet precipitation samples was likely derived from reactions transforming Hg^0 to Hg^{2+} (RGM or Hg_p) followed by scavenging into droplets or onto particle (aerosols) surfaces. Subsequent mainly physical processes are unlikely to produce MIF, we thus suggest that MIF of ^{200}Hg results from specific oxidation processes.

In the atmosphere, elemental Hg^0 can be oxidized into Hg^{2+} by oxidants such as ozone, H_2O_2, hydroxyl and halogen radicals (Morel et al., 1998; Schroeder et al., 1998; Lin and Pehkonen, 1999; Selin, 2009; O'Concubhair et al., 2012). Photo-oxidation of Hg^0 may occur also in natural water and snow (Lalonde et al., 2001). To elucidate the provenance of higher Δ^{200}Hg in samples with lower temperature (i.e. S1–S3, R1–R3, R20) and to clarify the impacts of air masses from different altitudes, we carried out a detailed investigation of air mass movements of these samples using the HYSPLIT back trajectory model. The calculations revealed a common phenomenon for these cold samples: whatever the movements of air masses in near surface layers, all samples displayed a downward transport of air mass from more than 6000 m AGL in the arctic region to the near surface layer (500 m AGL), while moving southward to Peterborough (see Supplementary Fig. S4). As the troposphere was shallower near the North Pole (i.e. 6000 m) and the transport probabilities of originally stratospheric air masses into the Arctic were highest in winter (Holton et al., 1995; James et al., 2003; Stohl et al., 2003), this suggests a sliding down of stratospheric air masses (containing Hg) along sloping isentropic surfaces at the "Arctic front" (constant temperature dome around the Arctic) into middle latitudes (i.e. Peterborough region). As the inter-layer between stratosphere and troposphere (tropopause) is rich in intense sunlight and ozone, an important oxidant with a long lifetime (10 days to 1 month) (Stohl et al., 2003; Lyman and Jaffe, 2012), we speculate that Δ^{200}Hg anomalies are likely related to intense sunlight irradiation and oxidant intensity. Sunlight fuels photolytic reactions and often plays an important role in atmospheric chemistry. We are only aware of one study reporting even Hg isotope anomalies triggered by photoreactions in compact fluorescence lamps (Mead et al., 2010), prompting us to relate ^{200}Hg MIF to the photolysis of Hg compounds. Likewise, MIF of sulfur isotopes produced during the photolysis of sulfur compounds has been suggested to exhibit a strong wavelength dependence (Farquhar et al., 2000, 2001). Hg mono-isotopic photosensitization has been studied since the 1950s. Photochemical oxidation of excited mercury atoms can enrich Hg up to 97% with the naturally least abundant isotope ^{196}Hg (Gunning, 1958; Viazovetski, 2005). These results were thought to be caused by wavelength-specific photo-excited reactions of chemical compounds, of which the specific electronic structure is only sensitive to specific absorption bands. The isotopic photosensitization effect on even Hg isotopes triggered by natural sunlight containing specific absorption bands, especially in the tropopause, cannot be ruled out, and simultaneously induced MIF of odd Hg isotopes cannot be excluded at this point. We suggest the photo-initiated chemical oxidation may probably induce a wavelength-dependent mass-independent isotopic effect causing MIF of ^{200}Hg in the tropopause.

As oxidant radicals have a relatively short lifetime, a special vector may be needed to capture these oxidants and Hg^0 together and thus promote the photo-initiated oxidation. We speculate the presence of aerosols or particles such as snow crystals may promote the photo-initiated Hg^0 oxidation causing Δ^{200}Hg anomalies. Previous studies showed the depletion of O_3 and Hg^0 in the Arctic requires both sunlight and frozen aerosol or snow surfaces (Lindberg et al., 2002). The fact that higher Δ^{200}Hg were found in snow samples and cold rain samples may suggest a strong impact of snow crystals and/or frozen aerosols that are present at the top of the troposphere and in the Arctic in winter. Bromide and chloride derived from sea salt evasion (O'Dowd and de Leeuw, 2007) are highly concentrated in the surface layer of frozen water droplets or snow crystals and strengthen the interaction between hydroxyl radicals and halogens to produce strongly oxidizing and reactive halogens (Foster et al., 2001; Lindberg et al., 2002). Moreover, it is well known that gaseous elemental Hg tends to adsorb readily on solid surfaces and especially on its own, new-formed compounds (i.e. HgO and Hg_2Cl_2) (Gunning, 1958; Lindberg et al., 2002). Hg_p was also determined in aerosols at 5–19 km, below and above the tropopause (Murphy et al., 1998). These complicated solid surfaces thus could serve as an appreciable vector where Hg^0 oxidation occurs. Given the dominant Hg^0 inventory of the atmosphere displayed close to zero or slightly negative Δ^{200}Hg (Gratz et al., 2010; Sherman et al., 2010), ^{200}Hg could preferentially be captured in products during the photo-initiated oxidation, creating positive Δ^{200}Hg in the much smaller RGM (and Hg_p) pool. The long aerosol lifetimes in the top troposphere could also allow for longer reaction times for photo-initiated oxidation, thus, producing higher Δ^{200}Hg anomalies (Holton et al., 1995; Stohl et al., 2003; James et al., 2003). In this study, all samples displayed an increasing trend of Δ^{200}Hg with Na (Fig. 6b). As Na is mainly derived from sea–salt aerosols (O'Dowd and de Leeuw, 2007), it again suggests an important role of halogen-enriched solid surfaces in producing Δ^{200}Hg anomalies. As a result, these particles serve not only as oxidation vectors, but also as an important oxidant source.

From late spring to early autumn, the occurrence of snow is very limited. The lower and relatively constant

Δ^{200}Hg anomalies may be linked to long-distance transport of Hg from the top troposphere layer, where only aerosols are available for this complex reaction. Frequent strong stratosphere to troposphere transports have been observed in middle latitude regions and stratosphere air can reside in the troposphere for several hours up to several days (Holton et al., 1995; James et al., 2003; Stohl et al., 2003; Lyman and Jaffe, 2012). These fluxes operate on long timescales and can probably penetrate deep (i.e. 6000 m altitude) into the troposphere of mid-latitude regions, having probably an important influence on Hg concentrations (Radke et al., 2007; Lyman and Jaffe, 2012) and Δ^{200}Hg anomalies in precipitation samples. In addition, the fact that ozone is more readily available relative to halogens in mid-latitude regions would support an additional reaction mechanism impacting MIF of ^{200}Hg.

As a result, Δ^{200}Hg anomalies could likely be a result of photo-initiated Hg^0 oxidation occurring on the surfaces of aerosols and particles in the tropopause. We should mention here that Hg^0 oxidation might fractionate other Hg isotopes as well. The formed RGM (and Hg_p) may penetrate deeply into the troposphere during stratosphere to troposphere transports and is apt to be scavenged into droplets or onto particle surfaces, inducing the observed Δ^{200}Hg anomalies in mid-latitude precipitation samples. Photochemical reactions of Hg occurring in the atmosphere boundary layer (<1000 m) may not induce significant even isotope MIF, likely explaining the absence of Δ^{200}Hg anomalies involved with polar atmospheric mercury depletion events (Sherman et al., 2010). Alternatively, reactions in the boundary layer may be complete oxidations, which then would not give rise to any fractionation. Only incomplete oxidation at higher altitudes would lead to even isotope anomalies. Although more work is needed to investigate the exact impact of temperature on producing Δ^{200}Hg anomalies, seasonal (and thus temperature) variation of Δ^{200}Hg may suggest an important role of snow crystals in winter, or alternatively the sensitivity of tropopause height to temperature changes that likely influence the frequency and depth of stratosphere intrusion (Stohl et al., 2003). Since only a relatively small fraction of the atmospheric Hg^0 pool gets oxidized at any given time, atmospheric Hg^0 would probably have only slightly negative Δ^{200}Hg MIF.

4. IMPLICATIONS OF MDF AND MIF OF ODD AND EVEN HG ISOTOPES

This study proposes that measurement of Hg isotope fractionation coupled with meteorological data may provide useful information for tracing atmospheric Hg sources. The reason why MIF of odd Hg isotopes derived from photoreduction of Hg in droplets is different from the heterogeneous reactions in snow still needs to be fully understood. All precipitation samples displayed significant positive MIF of ^{200}Hg and a clear seasonal variation of Δ^{200}Hg. We propose a conceptual model to explain possible processes causing Δ^{200}Hg anomalies. Future experiments and theoretical contribution are needed to fully understand the reaction mechanisms and pathways involved. Our results suggest that ^{200}Hg anomalies are likely related to stratosphere incursion, presence of aerosols, oxidant intensity, solar irradiation and air mass movement. As a result, MIF of ^{200}Hg could thus provide additional information about atmospheric chemistry and meteorological changes. Though the direct temperature effect on ^{200}Hg anomalies remains unknown, the seasonal (temperature) variation of Δ^{200}Hg is striking and may be a useful tool to help monitor related climate changes.

ACKNOWLEDGMENTS

We thank Y. Liu from CAS, H.-M. Bao from Louisiana State University, J. Gaillardet from IPG Paris, T. Bullen from USGS, X.-K. Zhu from CAGS and A. Galy from University of Cambridge for discussion. The authors acknowledge the associated editor D. Vance, reviewer J. Wiederhold and two anonymous reviewers who greatly improved the quality of the manuscript. J.-B. Chen was financially supported by Ontario Postdoctoral Fellowship and "hundred talents" project of Chinese Academy of Sciences.

APPENDIX A. SUPPLEMENTARY DATA

Supplementary data associated with this article can be found, in the online version, at http://dx.doi.org/10.1016/j.gca.2012.05.005.

REFERENCES

Ariya P. A. et al. (2004) The Arctic: a sink for mercury. *Tellus B* **56**, 397–403.

Bergquist B. A. and Blum J. D. (2007) Mass-dependent and -independent fractionation of Hg isotopes by photoreduction in aquatic systems. *Science* **318**, 417–420.

Bergquist B. A. and Blum J. D. (2009) The odds and evens of mercury isotopes: applications of mass-dependent and mass-independent isotope fractionation. *Elements* **5**, 353–357.

Biswas A., Blum J. D., Bergquist B. A., Keeler G. J. and Xie Z. (2008) Natural mercury isotope variation in coal deposits and organic soils. *Environ. Sci. Technol.* **42**, 8303–8309.

Blum J. D. and Bergquist B. A. (2007) Reporting of variations in the natural isotopic composition of mercury. *Anal. Bioanal. Chem.* **388**, 353–359.

Carignan J., Estrade N., Sonke J. E. and Donard O. F. X. (2009) Odd isotope deficits in atmospheric Hg measured in lichens. *Environ. Sci. Technol.* **43**, 5660–5664.

Chen J., Hintelmann H. and Dimock B. (2010) Chromatographic pre-concentration of Hg from dilute aqueous solutions for isotopic measurement by MC-ICP-MS. *J. Anal. At. Spectrom.* **25**, 1402–1409.

de Caritat P. et al. (2005) Chemical composition of arctic snow: concentration levels and regional distribution of major elements. *Sci. Total Environ.* **336**, 183–199.

Douglas T. A. and Sturm M. (2004) Arctic haze, mercury and the chemical composition of snow across northwestern Alaska. *Atmos. Environ.* **38**, 805–820.

Draxler R. R. and Rolph G. D. (2003) HYSPLIT (Hybrid Single Particle Lagrangian Integrated Trajectory. Model access via NOAA-ARL Website: http://ready.arl.noaa.gov/HYSPLIT.php.

Durnford D., Dastoor A., Figueras-Nieto D. and Ryjkov A. (2010) Long range transport of mercury to the Arctic and across Canada. *Atmos. Chem. Phys. Discuss.* **10**, 6063–6086.

Environment Canada, http://www.ec.gc.ca/.
Estrade N., Carignan J., Sonke J. E. and Donard O. F. X. (2009) Mercury isotope fractionation during liquid-vapor evaporation experiments. *Geochim. Cosmochim. Acta* **73**, 2693–2711.
Farquhar J., Bao H.-M. and Thiemens M. (2000) Atmospheric influence of earth's earliest sulfur cycle. *Science* **289**, 756–758.
Farquhar J., Savarino J., Airieau S. and Thiemens M. (2001) Observation of wavelength-sensitive mass-independent sulfur isotope effects during SO_2 photolysis: implications for the early atmosphere. *J. Geophys. Res.* **106**, 32829–32839.
Feng X., Foucher D., Hintelmann H., Yan H., He T. and Qiu (2010) Tracing mercury contamination sources in sediments using mercury isotope compositions. *Environ. Sci. Technol.* **44**, 3363–3368.
Foster K. L., Plastridge R. A., Bottenheim J. W., Shepson P. B., Finlayson-Pitts B. J. and Spicer C. W. (2001) The role of Br_2 and BrCl in surface ozone destruction at polar sunrise. *Science* **291**, 471–474.
Ghosh S., Xu Y., Humayun M. and Odom L. (2008) Mass-independent fractionation of mercury isotopes in the environment. *Geochem. Geophys. Geosyst.* **9**, Q03004. http://dx.doi.org/10.1029/2007gc001827.
Gratz L. E., Keeler G. J., Blum J. D. and Sherman L. S. (2010) Isotopic composition and fractionation of mercury in great lakes precipitation and ambient air. *Environ. Sci. Technol.* **44**, 7764–7770.
Gunning H. E. (1958) Primary processes in reactions initiated by photoexcited mercury isotopes. *Can. J. Chem. (Canada)* **36**, 89–95.
Hintelmann H. and Lu S. (2003) High precision isotope ratio measurements of mercury isotopes in cinnabar ores using multi-collector inductively coupled plasma mass spectrometry. *Analyst* **128**, 635–639.
Holton J. R., Haynes P. H., McIntyre M. E., Douglass A. R., Rood R. B. and Pfister L. (1995) Stratosphere–troposphere exchange. *Rev. Geophys.* **33**, 403–439.
Hoyer M., Burke J. and Keeler G. (1995) Atmospheric sources, transport and deposition of mercury in Michigan: two years of event precipitation. *Water Air Soil Pollut.* **80**, 199–208.
Jackson T. A., Whittle D. M., Evans M. S. and Muir D. C. G. (2008) Evidence for mass-independent and mass-dependent fractionation of the stable isotopes of mercury by natural processes in aquatic ecosystems. *Appl. Geochem.* **23**, 547–571.
Jaffe D., Prestbo E., Swartzendruber P., Weiss-Penzias P., Kato S., Takami A., Hatakeyama S. and Kajii Y. (2005) Export of atmospheric mercury from Asia. *Atmos. Environ.* **39**, 3029–3038.
James P., Stohl A., Forster C., Eckhardt S., Seibert P. and Frank A. (2003) A 15-year climatology of stratosphere–troposphere exchange with a Lagrangian particle dispersion model 2. Mean climate and seasonal variability. *J. Geophys. Res.* **108**(D12), 8522.
Kim K.-H., Ebinghaus R., Schroeder W. H., Blanchard P., Kock H. H., Steffen A., Froude F. A., Kim M.-Y., Hong S. and Kim J.-H. (2005) Atmospheric mercury concentrations from several observatory sites in the Northern Hemisphere. *J. Atmos. Chem.* **50**, 1–24.
Lalonde J. D., Amyot M., Kraepiel A. M. L. and Morel F. M. M. (2001) Photooxidation of Hg(0) in artificial and natural waters. *Environ. Sci. Technol.* **35**, 1367–1372.
Lalonde J. D., Poulain A. J. and Amyot M. (2002) The role of mercury redox reactions in snow on snow-to-air mercury transfer. *Environ. Sci. Technol.* **36**, 174–178.
Lalonde J. D., Amyot M., Doyon M.-R. and Auclair J.-C. (2003) Photo-induced Hg(II) reduction in snow from the remote and temperate Experimental Lakes Area (Ontario, Canada). *J. Geophys. Res.* **108**(D6), 4200.
Lamborg C. H., Rolfhus K. R., Fitzgerald W. F. and Kim G. (1999) The atmospheric cycling and air–sea exchange of mercury species in the South and equatorial Atlantic Ocean. *Deep Sea Res. Part II Top. Studies Oceanogr.* **46**, 957–977.
Landis M. S. and Keeler G. J. (2002) Atmospheric mercury deposition to Lake Michigan during the Lake Michigan mass balance study. *Environ. Sci. Technol.* **36**, 4518–4524.
Lauretta D. S., Klaue B., Blum J. D. and Buseek P. R. (2001) Mercury abundances and isotopic compositions in the Murchison (CM) and Allende (CV) carboneous chrondrites. *Geochim. Cosmochim. Acta* **65**, 2807–2818.
Lin C.-J. and Pehkonen S. O. (1999) The chemistry of atmospheric mercury: a review. *Atmos. Environ.* **33**, 2067–2079.
Lindberg S. E., Brooks S., Lin C. J., Scott K. J., Landis M. S., Stevens R. K., Goodsite M. and Richter A. (2002) Dynamic oxidation of gaseous mercury in the Arctic troposphere at polar sunrise. *Environ. Sci. Technol.* **36**, 1245–1256.
Lyman S. N. and Jaffe D. A. (2012) Formation and fate of oxidized mercury in the upper troposphere and lower stratosphere. *Nat. Geosci.* **5**, 114–117.
Macdonald R. W., Harner T. and Fyfe J. (2005) Recent climate change in the Arctic and its impact on contaminant pathways and interpretation of temporal trend data. *Sci. Total Environ.* **342**, 5–86.
Mason R. P., Fitzgerald W. F. and Morel F. M. M. (1994) The biogeochemical cycling of elemental mercury: anthropogenic influences. *Geochim. Cosmochim. Acta* **58**, 3191–3198.
Mead C., Anbar A. D. and Johnson T. M. (2010) *Mass-independent Fractionation of Hg Isotopes Resulting from Photochemical Self Shielding*. Goldshmidt, Knoxville, TN.
Morel F. o. M. M., Kraepiel A. M. L. and Amyot M. (1998) The chemical cycle and bioaccumulation of mercury. *Ann. Rev. Ecol. Syst.* **29**, 543–566.
Murphy D. M., Thomson D. S. and Mahoney M. J. (1998) In situ measurements of organics, meteoritic material, mercury, and other elements in aerosols at 5 to 19 kilometers. *Science* **282**, 1664–1669.
O'Concubhair R., O'Sullivan D. and SodeauDark J. R. (2012) Oxidation of dissolved gaseous mercury in polar ice mimics. *Environ. Sci. Technol.* **46**, 4829–4836.
O'Dowd C. D. and de Leeuw G. (2007) Marine aerosol production: a review of the current knowledge. *Philos. Trans. Roy. Soc. A Math. Phys. Eng. Sci.* **365**, 1753–1774.
Point D., Sonke J. E., Day R. D., Roseneau D. G., Hobson K. A., Vander Pol S. S., Moors A. J., Pugh R. S., Donard O. F. X. and Becker P. R. (2011) Methylmercury photodegradation influenced by sea-ice cover in Arctic marine ecosystems. *Nat. Geosci.* **4**, 188–194.
Radke L. F., Friedli H. R. and Heikes B. G. (2007) Atmospheric mercury over the NE Pacific during spring 2002: gradients, residence time, upper troposphere lower stratosphere loss, and long-range transport. *J. Geophys. Res.* **112**(D19), D19305.
Schauble E. A. (2007) Role of nuclear volume in driving equilibrium stable isotope fractionation of mercury, thallium, and other very heavy elements. *Geochim. Cosmochim. Acta* **71**, 2170–2189.
Schroeder W. H. and Munthe J. (1998) Atmospheric mercury – an overview. *Atmos. Environ.* **32**, 809–822.
Schroeder W. H., Anlauf K. G., Barrie L. A., Lu J. Y., Steffen A., Schneeberger D. R. and Berg T. (1998) Arctic springtime depletion of mercury. *Nature* **394**, 331–332.
Selin N. E. (2009) Global biogeochemical cycling of mercury: a review. *Ann. Rev. Environ. Resour.* **34**, 43–63.

Selin N. E. and Jacob D. J. (2008) Seasonal and spatial patterns of mercury wet deposition in the United States: constraints on the contribution from North American anthropogenic sources. *Atmos. Environ.* **42**, 5193–5204.

Sherman L. S., Blum J. D., Johnson K. P., Keeler G. J., Barres J. A. and Douglas T. A. (2010) Mass-independent fractionation of mercury isotopes in Arctic snow driven by sunlight. *Nat. Geosci.* **3**, 173–177.

Sherman L. S., Blum J. D., Keeler G. J., Demers J. D. and Timothy Dvonch J. (2012) Investigation of local mercury deposition from a coal-fired power plant using mercury isotopes. *Environ. Sci. Technol.* **46**, 382–390.

Sonke J. E. (2011) A global model of mass independent mercury stable isotope fractionation. *Geochim. Cosmochim. Acta* **75**, 4577–4590.

Stohl A., Bonasoni P., Cristofanelli P., Collins W., Feichter J., Frank A., Forster C., Gerasopoulos E., Geggeler H., James P., Kentarchos T., Kreipl S., Kromp-Kolb H., Kreger B., Land C., Meloen J., Papayannis A., Priller A., Seibert P., Sprenger M., Roelofs G. J., Scheel E., Schnabel C., Siegmund P., Tobler L., Trickl T., Wernli H., Wirth V., Zanis P. and Zerefos C. (2003) Stratosphere–troposphere exchange – a review, and what we have learned from STACCATO. *J. Geophys. Res.* **108**, 8516–8531.

Strode S. A., Jaegle L., Jaffe D. A., Swartzendruber P. C., Selin N. E., Holmes C. and Yantosca R. M. (2008) Trans-Pacific transport of mercury. *J. Geophys. Res.* **113**, D15305.

Travnikov O. (2005) Contribution of the intercontinental atmospheric transport to mercury pollution in the Northern Hemisphere. *Atmos. Environ.* **39**, 7541–7548.

US EPA, US Environment Protection Agency, http://www.epa.gov/. TRI Explorer: Releases: Trends Reports, 28 October 2010.

Viazovetski Y. (2005) Production of the Hg-196 isotope by a photochemical method. *Tech. Phys.* **50**, 347–350.

Wiederhold J. G., Cramer C. J., Daniel K., Infante I., Bourdon B. and Kretzschmar R. (2010) Equilibrium mercury isotope fractionation between dissolved Hg(II) species and thiol-bound Hg. *Environ. Sci. Technol.* **44**, 4191–4197.

Zheng W. and Hintelmann H. (2009) Mercury isotope fractionation during photoreduction in natural water is controlled by its Hg/DOC ratio. *Geochim. Cosmochim. Acta* **73**, 6704–6715.

Zheng W. and Hintelmann H. (2010a) Nuclear field shift effect in isotope fractionation of mercury during abiotic reduction in the absence of light. *J. Phys. Chem. A* **114**, 4238–4245.

Zheng W. and Hintelmann H. (2010b) Isotope fractionation of mercury during its photochemical reduction by low-molecular-weight organic compounds. *J. Phys. Chem. A* **114**, 4246–4253.

Zheng W., Foucher D. and Hintelmann H. (2007) Mercury isotope fractionation during volatilization of Hg (0) from solution into the gas phase. *J. Anal. At. Spectrom.* **9**, 1097–1104.

Associate editor: Derek Vance